

## NEW ABUNDANCE DETERMINATIONS OF CADMIUM, LUTETIUM, AND OSMIUM IN THE *r*-PROCESS ENRICHED STAR BD +17 3248 '

This article has been downloaded from IOPscience. Please scroll down to see the full text article.

2010 ApJ 714 L123

(<http://iopscience.iop.org/2041-8205/714/1/L123>)

The Table of Contents and more related content is available

Download details:

IP Address: 129.15.30.75

The article was downloaded on 07/04/2010 at 17:07

Please note that terms and conditions apply.

## NEW ABUNDANCE DETERMINATIONS OF CADMIUM, LUTETIUM, AND OSMIUM IN THE $r$ -PROCESS ENRICHED STAR BD +17 3248<sup>\*,†</sup>

IAN U. ROEDERER<sup>1</sup>, CHRISTOPHER SNEDEN<sup>1</sup>, JAMES E. LAWLER<sup>2</sup>, AND JOHN J. COWAN<sup>3</sup>

<sup>1</sup> Department of Astronomy, University of Texas at Austin, 1 University Station, C1400 Austin, TX 78712-0259, USA; iur@astro.as.utexas.edu

<sup>2</sup> Department of Physics, University of Wisconsin, Madison, WI 53706, USA

<sup>3</sup> Homer L. Dodge Department of Physics and Astronomy, University of Oklahoma, Norman, OK 73019, USA

Received 2010 March 8; accepted 2010 March 22; published 2010 April 6

### ABSTRACT

We report the detection of Cd I ( $Z = 48$ ), Lu II ( $Z = 71$ ), and Os II ( $Z = 76$ ) in the metal-poor star BD +17 3248. These abundances are derived from an ultraviolet spectrum obtained with the Space Telescope Imaging Spectrograph on the *Hubble Space Telescope*. This is the first detection of these neutron-capture species in a metal-poor star enriched by the  $r$  process. We supplement these measurements with new abundances of Mo I, Ru I, and Rh I derived from an optical spectrum obtained with the High Resolution Echelle Spectrograph on Keck. Combined with previous abundance derivations, 32 neutron-capture elements have been detected in BD +17 3248, the most complete neutron-capture abundance pattern in any metal-poor star to date. The light neutron-capture elements ( $38 \leq Z \leq 48$ ) show a more pronounced even-odd effect than expected from current solar system  $r$ -process abundance predictions. The age for BD +17 3248 derived from the Th II/Os II chronometer is in better agreement with the age derived from other chronometers than the age derived from Th II/Os I. New Hf II abundance derivations from transitions in the ultraviolet are lower than those derived from transitions in the optical, and the lower Hf abundance is in better agreement with the scaled solar system  $r$ -process distribution.

**Key words:** nuclear reactions, nucleosynthesis, abundances – stars: abundances – stars: individual (BD +17 3258, HD 122563) – stars: Population II

**Online-only material:** color figures

### 1. INTRODUCTION

Steady progress has been made over the last half-century toward understanding how the heaviest elements in the universe are produced. For the elements heavier than the iron (Fe) group, the vast majority of isotopes are produced by the successive addition of neutrons to existing nuclei on timescales that are slow or rapid relative to the average  $\beta^-$  decay rates. These are referred to as the slow ( $s$ ) and rapid ( $r$ ) neutron ( $n$ ) capture processes (see, e.g., Truran et al. 2002 and Sneden et al. 2008 for discussion of these processes). The basic physical principles of these reactions are well known. The  $s$ -process involves isotopes near the valley of  $\beta$  stability, so the properties relevant to understanding the nature of the  $s$ -process (e.g.,  $n$ -capture cross-sections, half-lives, etc.) can be studied in laboratories on Earth (see Cowan et al. 1991, and references therein). Phenomenological or nuclear reaction models can then be constructed to predict the general abundance pattern produced by the  $s$ -process (see Busso et al. 1999). When applied to the solar system (S.S.) heavy element abundance distribution, the  $s$ -process abundances can be subtracted from the total abundances to reveal the  $r$ -process component (e.g., Seeger et al. 1965; Kappeler et al. 1989; Arlandini et al. 1999). Due to the more energetic nature of the  $r$ -process and the exotic, short-lived nuclei involved,

reaction networks for the  $r$ -process were not tractable until only recently (see Kratz et al. 2007). To evaluate and verify detailed nucleosynthesis models, abundance patterns must be accurately characterized for as many elements as possible in locations beyond the S.S.

In this Letter, we report abundance estimates for neutral cadmium (Cd I,  $Z = 48$ ), singly ionized lutetium (Lu II,  $Z = 71$ ), and singly ionized osmium (Os II,  $Z = 76$ ) in the near-ultraviolet (NUV) spectrum of the  $r$ -process enriched metal-poor star BD +17 3248. This is the first clear detection of Cd and Lu in a metal-poor star enriched by the  $r$ -process. Combined with previous abundance derivations (Cowan et al. 2002, 2005; Sneden et al. 2009) and several other new abundances derived from the optical spectrum of this star, 32  $n$ -capture elements have been detected in BD +17 3248, the most complete  $n$ -capture pattern in any metal-poor star. In the metal-poor star HD 122563, which is relatively deficient in the heavy  $n$ -capture elements, we also report tentative detections for Cd I and Lu II, as well as an upper limit for Os II. Finally, we use these new abundances to differentiate among the various techniques used to predict the  $r$ -process abundance pattern.

### 2. OBSERVATIONS AND ABUNDANCE ANALYSIS

NUV spectra of BD +17 3248 and HD 122563 were obtained using the Space Telescope Imaging Spectrograph (STIS) on the *Hubble Space Telescope* (HST). These spectra cover a wavelength region from 2280 to 3120 Å at  $R \equiv \lambda/\Delta\lambda \sim 30,000$ . The optical spectrum of BD +17 3248 was obtained using the High Resolution Echelle Spectrograph (HIRES; Vogt et al. 1994) on Keck I, and this spectrum covers a wavelength region from 3120 to 4640 Å at  $R \sim 45,000$ . See Cowan et al. (2005) for further details.

\* Based on observations made with the NASA/ESA *Hubble Space Telescope*, obtained at the Space Telescope Science Institute, which is operated by the Association of Universities for Research in Astronomy, Inc., under NASA contract NAS 5-26555. These observations are associated with programs 8111 and 8342.

† Some of the data presented herein were obtained at the W. M. Keck Observatory, which is operated as a scientific partnership among the California Institute of Technology, the University of California, and the National Aeronautics and Space Administration. The Observatory was made possible by the generous financial support of the W. M. Keck Foundation.

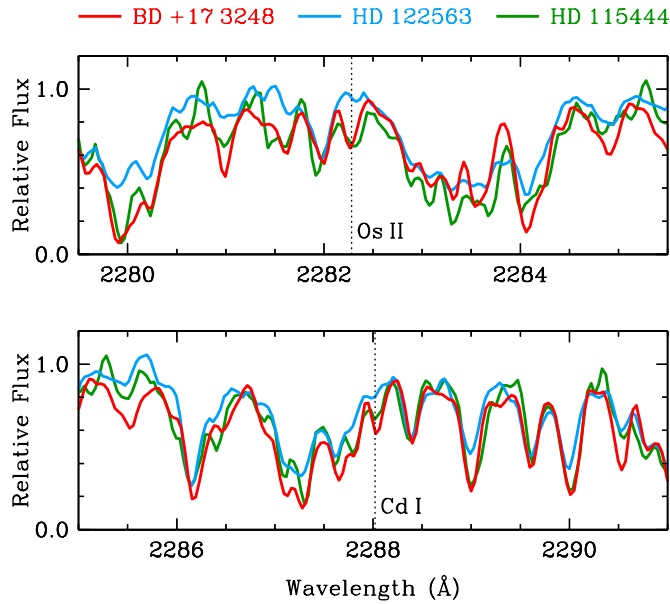


**Figure 1.** Spectral regions of BD +17 3248, HD 122563, and HD 115444 surrounding the Os II and Cd I lines. The spectra have been smoothed to increase their signal-to-noise ratios.

(A color version of this figure is available in the online journal.)

In Figure 1, we show segments of the STIS spectra surrounding the Os II transition at 2282.28 Å and the Cd I transition at 2288.02 Å in BD +17 3248 and HD 122563, as well as HD 115444.<sup>4</sup> A strong absorption feature is clearly identified at these wavelengths in BD +17 3248 but not in HD 122563. BD +17 3248 is warmer ( $T_{\text{eff}} = 5200$  K) and more metal-rich ( $[\text{Fe}/\text{H}] = -2.1$ ) than HD 122563 ( $T_{\text{eff}} = 4570$  K and  $[\text{Fe}/\text{H}] = -2.7$ ). HD 115444 has a temperature ( $T_{\text{eff}} = 4720$  K), metallicity ( $[\text{Fe}/\text{H}] = -2.9$ ), and overall light element abundance distribution (i.e.,  $6 \leq Z \leq 40$ ) that closely resembles HD 122563 (Westin et al. 2000). HD 115444 is overabundant in the heavy  $n$ -capture elements ( $[\text{Eu}/\text{Fe}] = +0.7$ ) relative to HD 122563 ( $[\text{Eu}/\text{Fe}] = -0.5$ ). Therefore, the only significant difference between the spectra of HD 115444 and HD 122563 should be the stronger heavy  $n$ -capture absorption lines in HD 115444. In Figure 1, we see that HD 115444, like BD +17 3248, also exhibits strong absorption features at 2282.28 and 2288.02 Å, but HD 122563 does not. Thus, heavy  $n$ -capture species must be producing this absorption. We find no transitions of heavy  $n$ -capture species at these wavelengths—or the Lu II line at 2615.41 Å—in the Kurucz or NIST line databases that could plausibly account for this absorption other than the species of interest.

References for published transition probabilities of the lines used in this analysis are given in Table 1. We determined the transition probability of the Lu II 2615.42 Å resonance line to be  $\log(gf) = +0.11 \pm 0.04$  based on a laser-induced fluorescence lifetime measurement of its upper level (Fedchak et al. 2000) and a branching fraction calculation of 0.971 (Quinet et al. 1999). (See also Lawler et al. 2009.) The  $^{175}\text{Lu}$  isotope is dominant (97.4% of S.S. Lu; Lodders 2003). The  $^{176}\text{Lu}$  isotope is blocked from  $r$ -process production by the stable  $^{176}\text{Yb}$  isotope, so it is expected to be entirely absent from BD +17 3248.

<sup>4</sup> This spectrum of HD 115444, taken with STIS using the same setup as the spectra of BD +17 3248 and HD 122563, has considerably lower signal-to-noise ratio, and we do not examine HD 115444 beyond this initial test.

**Table 1**  
Derived Stellar Abundances

Species	Z	$\lambda$ (Å)	E.P. (eV)	$\log(gf)$	Ref.	BD +17 3248 $\log \epsilon$	HD 122563 $\log \epsilon$
New Abundances from STIS Spectra							
Cd I	48	2288.02	0.00	+0.15	1	-0.03	-2.10
Lu II	71	2615.41	0.00	+0.11	2	-1.58	-2.96
Hf II <sup>a</sup>	72	2638.72	0.00	-0.17	3	-0.62	...
Hf II <sup>a</sup>	72	2641.41	1.04	+0.57	3	-0.91	...
Hf II <sup>a</sup>	72	2820.23	0.38	-0.05	3	-0.77	...
Hf II <sup>a</sup>	72	3012.90	0.00	-0.60	3	-0.74	...
Os II	76	2282.28	0.00	-0.14	4	+0.03	< -1.56
New Abundances from HIRES Spectra							
Nb II	41	3215.59	0.44	-0.24	5	-0.26	...
Mo I	42	3864.10	0.00	-0.01	6	+0.17	...
Ru I	44	3498.94	0.00	+0.31	7	+0.34	...
Rh I	45	3434.89	0.00	+0.45	8	-0.57	...
Pd I <sup>a</sup>	46	3242.70	0.81	+0.07	9	-0.10	...
Pd I <sup>a</sup>	46	3404.58	0.81	+0.33	9	-0.09	...
Pd I <sup>a</sup>	46	3516.94	0.94	-0.21	9	+0.05	...
Ag I <sup>a</sup>	47	3280.67	0.00	-0.04	10	-0.83	...
Ag I <sup>a</sup>	47	3382.90	0.00	-0.35	10	-0.67	...

**Notes.**

<sup>a</sup> The mean abundances in BD +17 3248 are  $\log \epsilon (\text{Ag I}) = -0.75 \pm 0.14$ ,  $\log \epsilon (\text{Pd I}) = -0.05 \pm 0.09$ , and  $\log \epsilon (\text{Hf II}) = -0.76 \pm 0.14$ .

**References.** (1) Morton 2000; (2) this study; (3) Lawler et al. 2007; (4) Ivarsson et al. 2004; (5) Nilsson et al. 2010; (6) Whaling & Brault 1988; (7) Wickliffe et al. 1994; (8) Kwiatkowski et al. 1982; (9) Xu et al. 2006; (10) Fuhr & Wiese 2009.

The odd- $Z$  isotope  $^{175}\text{Lu}$  has nonzero nuclear spin  $I = 7/2$ . Hyperfine structure (hfs) and an accurate line position are based on new laboratory measurements of the  $6s6p \ ^1P^0$  level energy,  $38223.406(8) \text{ cm}^{-1}$ , hfs A,  $-0.03731(10) \text{ cm}^{-1}$ , and hfs B,  $0.0811(15) \text{ cm}^{-1}$ . The naturally occurring  $r$ -process isotopes of Cd and Os are predominantly even- $Z$  even- $N$  isotopes with zero nuclear spin, thus we are justified in ignoring the hfs from their minority isotopes.

We use the current version of the LTE spectral analysis code MOOG (Sneden 1973) to perform the abundance analysis. We adopt the atmospheric parameters for BD +17 3248 and HD 122563 derived by Cowan et al. (2002) and Simmerer et al. (2004) ( $T_{\text{eff}}/\log g/[\text{M}/\text{H}]/v_t = 5200 \text{ K}/1.80/-2.08/1.9 \text{ km s}^{-1}$  and  $4570 \text{ K}/1.35/-2.50/2.9 \text{ km s}^{-1}$ , respectively) and interpolate model atmospheres from the Kurucz grids (Castelli et al. 1997).

We compare our results to abundances of other species derived from lines in the optical spectral range. In the NUV, bound-free continuous opacity from metals may be comparable to or greater than the bound-free continuous opacity from  $\text{H}^-$  that dominates in the optical spectral range for metal-poor stars (e.g., Travis & Matsushima 1968). To compensate for deficiencies in our ability to model the continuous opacity in this spectral range, we have derived abundances of relatively clean, unsaturated, and unblended Fe I and Zr II lines across the NUV. We require that these lines have reliable  $\log(gf)$  values (Fe I: O'Brian et al. 1991 or a grade of "C" or better in the NIST database; Zr II: Malcheva et al. 2006), and we derive the abundances by matching synthetic to observed spectra. Ideally we should select metals that make significant contributions to the continuous opacity (e.g., Mg, as advocated by Bell et al. 2001), but practically we are constrained because there are very few metals whose lines have reliable laboratory transition

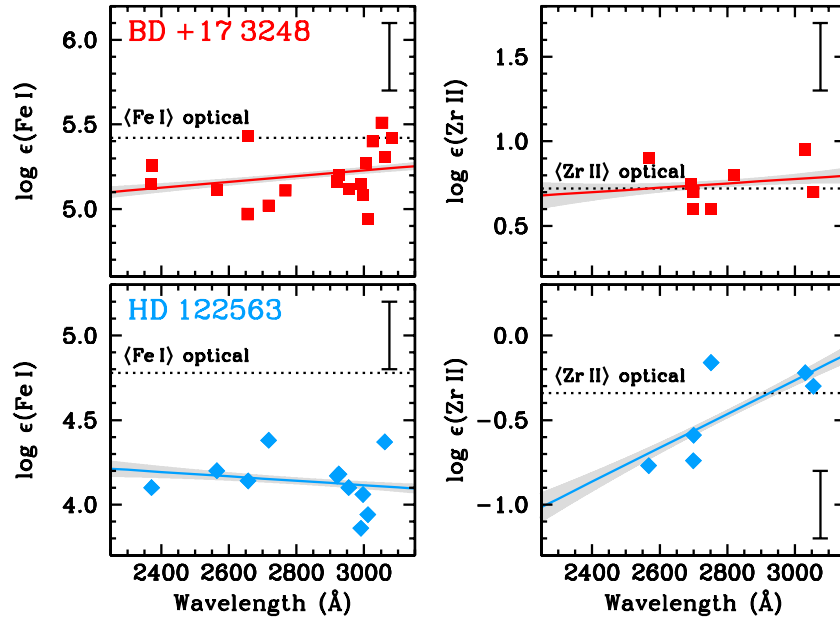


**Figure 2.** Abundances derived from NUV transitions of Fe I and Zr II in BD +17 3248 and HD 122563. A representative  $1\sigma$  abundance uncertainty for each transition is illustrated. The solid lines represent linear fits to the abundances, with uncertainties indicated by the shaded regions. The mean abundance of each species derived from transitions in the optical spectral range is indicated by the dotted lines. Abundances have been renormalized to a common  $\log(gf)$  scale in both stars, and the Zr II abundance in HD 122563 has been renormalized to the Zr II (optical) abundance using the equivalent width measurements of Honda et al. (2004) to account for the different model atmosphere parameters between Honda et al. (2006) and the present study.

(A color version of this figure is available in the online journal.)

probabilities and are unsaturated and unblended in the NUV spectra of these stars.

Figure 2 displays the abundances of Fe I and Zr II in BD +17 3248 and HD 122563 as a function of wavelength. Two characteristics would indicate that we have successfully reproduced the continuous opacity: (1) no trend between abundance and wavelength and (2) agreement between the abundances derived from the optical and NUV transitions. A similar phenomenon is observed in both BD +17 3248 and HD 122563. For Fe I, we detect both an offset and a very slight trend in both stars, though the effect is much smaller in BD +17 3248, the warmer of the two stars. There is no offset and only a minimal trend for Zr II in BD +17 3248, but a much larger trend is observed in HD 122563, although we have only derived abundances from six Zr II lines. We use these trends as “local metallicity” references to empirically adjust the derived abundances of other species (where neutral species are adjusted according to Fe I and singly ionized species are adjusted according to Zr II). For example, the abundance derived from the Cd I line at 2615 Å in BD +17 3248 is adjusted by +0.32 dex, the difference between a hypothetical Fe I line at 2615 Å and the mean Fe I abundance for lines in the optical spectral region. We caution that there are very few Fe I lines and no Zr II lines shortward of the Mg I series limit at 2515 Å, where the bound-free opacity contribution from Mg I may increase substantially. This uncertainty should be borne in mind when extrapolating the trends to shorter wavelengths.

We derive the abundances of Cd I, Lu II, and Os II in BD +17 3248 by comparing synthetic spectra to the observed absorption profiles. These fits are shown in Figure 3, and the adjusted abundances are reported in Table 1. In HD 122563 we report the tentative detection of Cd I and Lu II, but we can only estimate an upper limit for Os II. The Os II line is relatively unblended in BD +17 3248. The Cd I line is blended with an Fe I transition at 2288.04 Å and an As I transition at 2288.12 Å. Unfortunately, neither has a laboratory  $\log(gf)$  measurement, so we are forced

to fit these blends as best as possible. The continuum is depressed slightly at the Lu II line in HD 122563 and more substantially in BD +17 3248 by saturated Fe II lines at 2613.82 and 2617.62 Å. Furthermore, this line is contaminated with OH in HD 122563, although this blend is minimized in the warmer atmosphere of BD +17 3248. Considering all of these sources of uncertainty in the fits and the corrections to account for the continuous opacity, we estimate an uncertainty of at least 0.30 dex for each abundance derivation.

We have rederived the Hf II abundance in BD +17 3248 using four transitions in the NUV. Several Hf II transitions can also be detected in the optical spectral range. Finally, we have derived new or revised abundances for several elements between the first and second *r*-process peaks in BD +17 3248 (Nb, Mo, Ru, Rh, Pd, and Ag;  $Z = 41$ – $42$  and  $44$ – $47$ ) using the Keck spectrum. These abundances are reported in Table 1.

### 3. RESULTS AND DISCUSSION

In Figure 4, we display the abundance distribution for the *n*-capture elements in BD +17 3248. The S.S. *r*-process abundance distribution, calculated as residuals from a classical model of the *s*-process (Snedden et al. 2008), is shown for comparison. When normalized to the Eu abundance in BD +17 3248, this distribution is a superb match to the stellar abundances for  $Z \geq 56$ , as has been demonstrated previously (e.g., Cowan et al. 2002).

The detection of Cd extends the suite of lighter *n*-capture elements observed in metal-poor stars more than halfway between the first and second *r*-process peaks (roughly  $A \sim 80$  and 130, respectively). For Sr to Cd ( $Z = 38$ – $48$ , missing only the short-lived isotopes of Tc,  $Z = 43$ ), there is a very pronounced even–odd abundance pattern in BD +17 3248, much more so than is predicted by the scaled S.S. *r*-process distribution or the *r*-process residuals derived from the (solar metallicity)

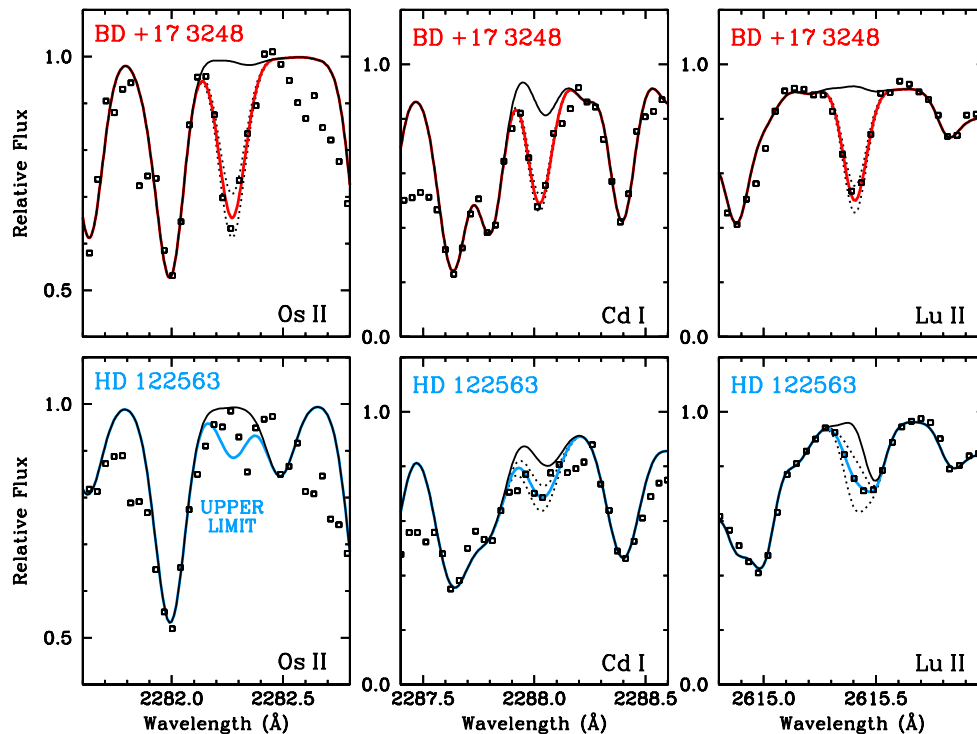


**Figure 3.** Fits of synthetic spectra to the observed spectra in BD +17 3248 and HD 122563. The bold lines indicate the best fit, dotted lines indicate  $\pm 0.30$  dex from the best fit, and the thin line indicates a synthesis with the species of interest removed.

(A color version of this figure is available in the online journal.)

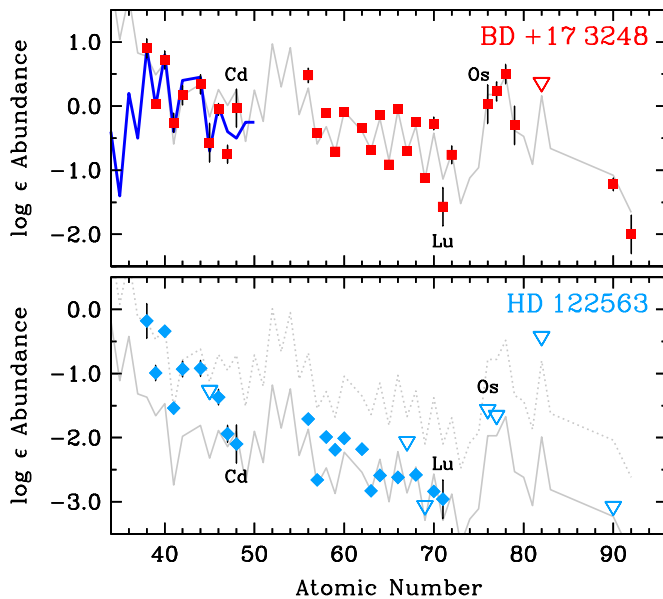


**Figure 4.** Neutron-capture abundance distributions in BD +17 3248 and HD 122563. Detections are indicated by filled symbols and upper limits are indicated by downward-facing open triangles. The bold blue line in the top panel represents the core collapse supernova high-entropy neutrino wind calculations of Farouqi et al. (2009, estimated from their Figure 3), normalized to Sr ( $Z = 38$ ). The solid line in each panel represents the scaled S.S.  $r$ -process abundance distribution (Sneden et al. 2008), normalized to Eu ( $Z = 63$ ), and the dotted line in the lower panel represents this same distribution normalized instead to Sr. Abundances are taken from Cowan et al. (2002, 2005), Honda et al. (2006), Roederer et al. (2009), Sneden et al. (2009), and the present study. Several elements have been renormalized to a common set of laboratory  $\log(gf)$  values, and the abundances of HD 122563 have been renormalized to our abundance scale as described in the caption of Figure 2.

(A color version of this figure is available in the online journal.)

stellar  $s$ -process model of Arlandini et al. 1999 (not shown). This effect was first noticed in the Pd and Ag abundance pattern of three  $r$ -process enriched stars observed by Johnson & Bolte (2002). The large-scale dynamical network calculations from the core collapse supernova high-entropy neutrino wind model of Farouqi et al. (2009) reproduce this pattern better for Sr–Pd but still underestimate the even–odd effect for Ag and Cd. This general agreement is encouraging, but additional calculations and comparisons are warranted.

Lu is the final member of the rare earth elements (REE) to be unambiguously detected in  $r$ -process enriched metal-poor stars. The Lu/Eu (or, more generally, Lu/REE) ratio predicted by the scaled S.S.  $r$ -process distribution is in reasonable, though not perfect, agreement with our derived Lu abundance. Additional Lu abundance derivations for other metal-poor,  $r$ -process enhanced stars are required to assess whether the predicted Lu abundance or the stellar measurement (or both) is in error.

Each of the neutral and singly ionized states of Os have now been detected in BD +17 3248, and our abundance of Os II,  $\log \epsilon = +0.03$ , is in fair agreement with an updated Os I abundance derived from three optical and NUV lines,  $\log \epsilon = +0.25$ . Os is the heaviest stable element that can be detected in its singly ionized state in BD +17 3248. If the Os II abundance should prove reliable and its uncertainty can be reduced, this has the potential to offer two significant improvements for nuclear cosmochronometry. The only radioactive isotopes practical for age dating the material in old stars are  $^{232}\text{Th}$  and  $^{238}\text{U}$ , both of which can only be detected as first ions. Abundance uncertainties are minimized when considering ratios of two elements in the same ionization state. When predicting the initial production ratios, the uncertainty is generally smallest when the two elements are as close in mass number as possible. Previously, the heaviest singly ionized reference element has been Hf II, whose

stable isotopes are separated by 52–55 mass units from  $^{232}\text{Th}$ ; the stable *r*-process isotopes of Os are only separated by 40–44 mass units from  $^{232}\text{Th}$ . Adopting the range of production ratios from Kratz et al. (2007), the  $\text{Th II/Os II}$  ratio predicts an age range of 15.7–21.5 Gyr, whereas  $\text{Th II/Os II}$  predicts an age range of 5.4–11.2 Gyr. The latter is in better agreement with the age predicted from other chronometer pairs (e.g.,  $\text{Th II/Eu II}$ , which predicts an age range of 7.9–12.3 Gyr). The present uncertainty in our Os II abundance translates to an age precision of 14 Gyr, but if the Os II uncertainty could be reduced to 0.10 dex the age precision would improve to 4.7 Gyr.

The Hf II abundance derived in BD +17 3248 from four lines in the NUV is marginally lower ( $\log \epsilon = -0.76 \pm 0.08$ ,  $\sigma = 0.14$ ) than that derived from six lines in the optical ( $\log \epsilon = -0.57 \pm 0.03$ ,  $\sigma = 0.08$ ). Previous analyses of the Hf II abundance in *r*-process enriched metal-poor stars have revealed that the stellar Hf II *r*-process abundance is higher by 0.15–0.25 dex than that predicted by the scaled S.S. *r*-process distribution (Lawler et al. 2007; Roederer et al. 2009; Sneden et al. 2009). Our Hf II NUV abundance is in excellent agreement with the scaled S.S. *r*-process Hf/REE ratio. Many of the transitions used to derive the REE stellar *r*-process abundance distribution from the optical spectral range arise from 0.0 eV lower levels, but only one of the 12 Hf II lines employed by Lawler et al. (2007) has a 0.0 eV lower level. Two of the four lines used to derive our NUV Hf II abundance arise from 0.0 eV levels, with  $\log \epsilon = -0.68$  from just these two transitions. Perhaps by using these transitions we have mitigated a subtle systematic effect present in the computation of the Hf II abundance relative to other REE. This might imply that other stellar Hf II *r*-process abundances—rather than the predicted S.S. *r*-process abundances—warrant minor revisions. Again adopting the range of production ratios from Kratz et al. (2007), the NUV  $\text{Th II/Hf II}$  ratio predicts an age range of 5.8–18.5 Gyr, whereas the optical  $\text{Th II/Hf II}$  ratio predicts an age of 14.7–27.4 Gyr. The precision is 5–6 Gyr in each measurement, but clearly the lower Hf II abundance derived from the NUV lines provides a more realistic age estimate for BD +17 3248.

Figure 4 also displays the abundance distribution for HD 122563, which is known to be deficient in the heavy *n*-capture elements. The scaled S.S. *r*-process distribution is a poor fit to the abundance pattern whether normalized to the first *r*-process peak or the REE (Honda et al. 2006). (No reasonable *s*-process distribution, or combination of *r*- and *s*-process distributions, matches either.) HD 122563 may be an example of enrichment by the so-called “weak” *r*-process, which produces small amounts of light *n*-capture material and steadily decreasing amounts of heavier material (Honda et al. 2006; Wanajo & Ishimaru 2006). Our Cd abundance in HD 122563 suggests that the downward abundance trend continues in the region between the first and second *r*-process peaks. Our Os upper limit in this star is not strong enough to exclude a scaled S.S. *r*-process pattern between the REE and the third *r*-process peak.

The detection of these three new species in BD +17 3248 is only a first step in understanding how and in what amount these elements were produced. By examining their abundances in other metal-poor stars enriched to different levels by the *r*-process, we may gain a better sense of any systematic offsets affecting the present analysis. These uncertainties must be minimized to take full advantage of these species as constraints on *n*-capture nucleosynthesis models and meaningful age probes for the *n*-capture material in metal-poor stars.

We thank the referee, David Lai, for a careful review of the manuscript. The authors recognize and acknowledge the very significant cultural role and reverence that the summit of Mauna Kea has always had within the indigenous Hawaiian community. We are most fortunate to have the opportunity to conduct observations from this mountain. This research has made use of the NASA Astrophysics Data System (ADS) and the NIST Atomic Spectra Database. Funding for this project has been generously provided by the U.S. National Science Foundation (grants AST 09-08978 to C.S., AST 09-07732 to J.E.L., and AST 07-07447 to J.J.C.).

*Facilities:* HST (STIS), Keck:I (HIRES)

## REFERENCES

- Arlandini, C., Käppeler, F., Wisshak, K., Gallino, R., Lugaro, M., Busso, M., & Straniero, O. 1999, *ApJ*, **525**, 886
- Bell, R. A., Balachandran, S. C., & Bautista, M. 2001, *ApJ*, **546**, L65
- Busso, M., Gallino, R., & Wasserburg, G. J. 1999, *ARA&A*, **37**, 239
- Castelli, F., Gratton, R. G., & Kurucz, R. L. 1997, *A&A*, **318**, 841
- Cowan, J. J., Thielemann, F.-K., & Truran, J. W. 1991, *Phys. Rep.*, **208**, 267
- Cowan, J. J., et al. 2002, *ApJ*, **572**, 861
- Cowan, J. J., et al. 2005, *ApJ*, **627**, 238
- Farouqi, K., Kratz, K.-L., Mashonkina, L. I., Pfeiffer, B., Cowan, J. J., Thielemann, F.-K., & Truran, J. W. 2009, *ApJ*, **694**, L49
- Fedchak, J. A., Den Hartog, E. A., Lawler, J. E., Palmeri, P., Quinet, P., & Biémont, E. 2000, *ApJ*, **542**, 1109
- Fuhr, J. R., & Wiese, W. L. 2009, in *Atomic Transition Probabilities*, Published in the CRC Handbook of Chemistry and Physics, ed. D. R. Lide (90th ed.; Boca Raton, FL: CRC Press, Inc.)
- Honda, S., Aoki, W., Ishimaru, Y., Wanajo, S., & Ryan, S. G. 2006, *ApJ*, **643**, 1180
- Honda, S., et al. 2004, *ApJS*, **152**, 113
- Ivarsson, S., Wahlgren, G. M., Dai, Z., Lundberg, H., & Leckrone, D. S. 2004, *A&A*, **425**, 353
- Johnson, J. A., & Bolte, M. 2002, *ApJ*, **579**, 616
- Käppeler, F., Beer, H., & Wisshak, K. 1989, *Rep. Prog. Phys.*, **52**, 945
- Kratz, K.-L., Farouqi, K., Pfeiffer, B., Truran, J. W., Sneden, C., & Cowan, J. J. 2007, *ApJ*, **662**, 39
- Kwiatkowski, M., Zimmermann, P., Biémont, E., & Grevesse, N. 1982, *A&A*, **112**, 337
- Lawler, J. E., den Hartog, E. A., Labby, Z. E., Sneden, C., Cowan, J. J., & Ivans, I. I. 2007, *ApJS*, **169**, 120
- Lawler, J. E., Sneden, C., Cowan, J. J., Ivans, I. I., & Den Hartog, E. A. 2009, *ApJS*, **182**, 51
- Lodders, K. 2003, *ApJ*, **591**, 1220
- Malcheva, G., Blagoev, K., Mayo, R., Ortiz, M., Xu, H. L., Svanberg, S., Quinet, P., & Biémont, E. 2006, *MNRAS*, **367**, 754
- Morton, D. C. 2000, *ApJS*, **130**, 403
- Nilsson, H., et al. 2010, *A&A*, **511**, A16
- O’Brian, T. R., Wickliffe, M. E., Lawler, J. E., Whaling, W., & Brault, J. W. 1991, *J. Opt. Soc. Am. B: Opt. Phys.*, **8**, 1185
- Quinet, P., Palmeri, P., Biémont, E., McCurdy, M. M., Rieger, G., Pinnington, E. H., Wickliffe, M. E., & Lawler, J. E. 1999, *MNRAS*, **307**, 934
- Roederer, I. U., Kratz, K.-L., Frebel, A., Christlieb, N., Pfeiffer, B., Cowan, J. J., & Sneden, C. 2009, *ApJ*, **698**, 1963
- Seeger, P. A., Fowler, W. A., & Clayton, D. D. 1965, *ApJS*, **11**, 121
- Simmerer, J., Sneden, C., Cowan, J. J., Collier, J., Woolf, V. M., & Lawler, J. E. 2004, *ApJ*, **617**, 1091
- Sneden, C. A. 1973, PhD thesis, Univ. of Texas at Austin
- Sneden, C., Cowan, J. J., & Gallino, R. 2008, *ARA&A*, **46**, 241
- Sneden, C., Lawler, J. E., Cowan, J. J., Ivans, I. I., & Den Hartog, E. A. 2009, *ApJS*, **182**, 80
- Travis, L. D., & Matsushima, S. 1968, *ApJ*, **154**, 689
- Truran, J. W., Cowan, J. J., Pilachowski, C. A., & Sneden, C. 2002, *PASP*, **114**, 1293
- Vogt, S. S., et al. 1994, *Proc. SPIE*, **2198**, 362
- Wanajo, S., & Ishimaru, Y. 2006, *Nucl. Phys. A*, **777**, 676
- Westin, J., Sneden, C., Gustafsson, B., & Cowan, J. J. 2000, *ApJ*, **530**, 783
- Whaling, W., & Brault, J. W. 1988, *Phys. Scr.*, **38**, 707
- Wickliffe, M. E., Salih, S., & Lawler, J. E. 1994, *J. Quant. Spectrosc. Radiat. Transfer*, **51**, 545
- Xu, H. L., Sun, Z. W., Dai, Z. W., Jiang, Z. K., Palmeri, P., Quinet, P., & Biémont, É. 2006, *A&A*, **452**, 357